

Published in final edited form as:

*Science*. 2014 July 11; 345(6193): 222–5. doi:10.1126/science.1253089.

## A Doppler Effect in Embryonic Pattern Formation

Daniele Soroldoni<sup>#1,3,4</sup>, David J. Jörg<sup>#2</sup>, Luis G. Morelli<sup>1,5</sup>, David L. Richmond<sup>1</sup>, Johannes Schindelin<sup>2,6</sup>, Frank Jülicher<sup>2</sup>, Andrew C. Oates<sup>1,3,4,\*</sup>

<sup>1</sup>Max Planck Institute of Molecular Cell Biology and Genetics, Pfotenhauerstr. 108, 01307 Dresden, Germany

<sup>2</sup>Max Planck Institute for the Physics of Complex Systems, Nöthnitzer Str. 38, 01187 Dresden, Germany

<sup>3</sup>MRC-National Institute for Medical Research, The Ridgeway, Mill Hill, London, NW7 1AA, UK

<sup>4</sup>University College London, Gower Street, London, WC1E 6BT, UK

<sup>5</sup>Departamento de Física, FCEyN UBA and IFIBA, CONICET; Pabellón 1, Ciudad Universitaria, 1428 Buenos Aires, Argentina

<sup>6</sup>University of Wisconsin at Madison, LOCI, 271 Animal Sciences 1675 Observatory Drive, Madison, WI 53706, USA

# These authors contributed equally to this work.

### Abstract

During embryonic development, temporal and spatial cues are coordinated to generate a segmented body axis. In sequentially segmenting animals, the rhythm of segmentation is reported to be controlled by the time-scale of genetic oscillations that periodically trigger new segment formation. However, we present real-time measurements of genetic oscillations in zebrafish embryos showing that their time-scale is not sufficient to explain the temporal period of segmentation. A second time-scale, the rate of tissue shortening, contributes to the period of segmentation through a Doppler effect. This contribution is modulated by a gradual change in the oscillation profile across the tissue. We conclude that the rhythm of segmentation is an emergent property controlled by the time-scale of genetic oscillations, the change of oscillation profile, and tissue shortening.

---

Segmental patterns are common throughout nature. In animals from diverse phyla, segmentation of the body axis occurs during embryogenesis, and in most cases, segments are added sequentially with a distinct period as the body axis elongates. Recent findings indicate that a common mechanism involving genetic oscillations underlies this morphological segmentation in vertebrates and arthropods (1). Here we ask how the time-scale of genetic oscillations determines the timing of segmentation.

---

\*correspondence to aoates@nimr.mrc.ac.uk.

**Author contributions:** DS, DJ, LGM, ACO designed experiments; DS performed experiments; JS developed analysis tools; DS, DJ, LGM, ACO analysed data; DS, DJ, DLR, LGM, FJ, ACO developed the concepts and wrote the paper.

In sequentially segmenting animals, the unsegmented tissue exhibits patterns of oscillating gene expression reminiscent of waves that travel from the posterior to the anterior where they arrest. These waves are kinematic and emerge at the tissue level from the coordinated output of cellular genetic oscillators (2–5). This situation is similar to news ticker displays where a moving pattern is caused by on-and-off switching of individual stationary lamps (6). The sequential arrest of the kinematic waves is thought to prefigure the position and set the period of segment formation (7). During vertebrate segmentation, the onset and arrest of these waves is controlled by a complex genetic network that acts in the unsegmented pre-somitic mesoderm (PSM). The PSM gives rise to the somites, which are the precursors of adult segments (vertebrae, ribs and associated skeletal muscles). Since its discovery, it has been generally assumed that this network, termed the “segmentation clock”, resembles a genetic clock with a single, well-defined period (3). In this simplified picture, both the onset and arrest of the kinematic waves happen with the same period, which is identical to that of segment formation (6–9). However, these fundamental assumptions have not been tested systematically because it has proven difficult to visualize oscillating gene expression in real-time and simultaneously quantify the timing of morphological segmentation over a significant timescale (2, 4, 10).

To this end, we used a transgenesis approach to generate a reliable reporter for the oscillating gene *her1*, named *Looping* (Fig. S1) and developed a multidimensional time-lapse set-up designed to systematically compare the periods of morphological segmentation and genetic oscillations in multiple zebrafish embryos (Fig. 1A). Our imaging set-up was sensitive enough to detect reporter oscillations in real-time and fast enough to simultaneously record segment formation in a population of 20 embryos (Fig. 1B and movie S1). Embryonic growth was not affected by our mounting technique, which ensured that wildtype and transgenic siblings developed normally (Fig. S2). With this approach, we observed that multiple kinematic waves (color arrowheads in Fig. 1C and movie S1) travel from the posterior to anterior PSM at each point in time. As expected, we found that the arrest of reporter oscillations in the anterior PSM coincided with the formation of every new segment (arrowhead in Fig. 1B and movie S2) (2, 7, 11). As the waves travel along the tissue, their wavelength shortens (arrows Fig. 1C), thus the wave pattern can be characterized by the number of waves and by their wavelengths.

To quantify the timing of onset and arrest of kinematic waves, we locally measured the reporter expression in the anterior and the posterior PSM (circles in Fig. 1D). From previous studies it was unclear whether the posterior PSM oscillates (2, 12). We found that both regions oscillate, although with different reporter amplitudes (Fig. 1D, lower diagram). We found that within the same time interval the number of oscillations in the posterior was smaller than in the anterior: during 9 posterior oscillations, 10 oscillations occur in the anterior (Fig. 1d). Consequently, oscillations in the posterior are slower with an average offset of about 9% ( $8.8 \pm 0.52\%$ ,  $p < 0.0001$ , Fig. 1E). This finding is not consistent with a single, well-defined period for the “segmentation clock”. Next, we directly compared the periods of genetic oscillations and segment formation, focusing on trunk segmentation where the segmentation period is known to be constant (13). We found that the period of anterior oscillations is the same as segmentation (Fig. 1E). Thus, the period of segmentation matches the period with which kinematic waves arrest in the anterior, but is significantly

faster than the period of genetic oscillations in the posterior (Fig. 1E): during 9 posterior oscillations, 10 segments are formed.

To understand this paradoxical period offset we aimed to obtain a comprehensive picture of reporter expression throughout the PSM. To this end, we generated kymographs that display the average reporter intensity along lines of interest (LOI) throughout the entire PSM (Fig. 2A). Each horizontal line of pixels in this kymograph represents a LOI at a specific time point and its length corresponds to the PSM length. Obvious features of all kymographs are the trajectories of kinematic waves and the substantial shortening of the PSM over time (average total shortening 60% after 13 segments). This implies the relative motion of the anterior end of the PSM, where the waves arrest, towards the posterior end. As a consequence, the anterior end moves into the approaching kinematic waves, shortening the time interval between their onset and arrest. This is reminiscent of the Doppler effect, in which an observer moving towards a sound source perceives an increased sound frequency compared to an observer at rest.

In the presence of a Doppler effect, the number of kinematic waves decreases as the tissue shortens (Supplementary text). To test this expectation, we analyzed the spatio-temporal properties of kinematic waves for a population of embryos by generating phase maps from the intensity kymographs (Fig. 2B and C; Fig. S3; Supplementary Text). These phase maps capture the spatial and temporal dynamics of oscillations while being independent of local amplitude variations (Fig. 2B). A horizontal line of pixels in the phase map captures the profile of phases at a specific time point (yellow line, Fig. 2C); a phase increment of  $2\pi$  along a horizontal line corresponds to one kinematic wave and the distance covered by this increment is the local wavelength (pink ticks, Fig. 2C; movie S3). Therefore, the number of kinematic waves can be determined by the antero-posterior phase difference divided by  $2\pi$ . These phase maps can be used to determine whether the number of kinematic waves changes over time with a sub-integer resolution exceeding that of simple peak counting in a kymograph. We found that the average number of kinematic waves decreases with the number of formed segments (Fig. 2D; movie S4, S5). Consistent with this analysis, a decrease in the number of kinematic waves can also be observed from snapshots of endogenous oscillating genes in wildtype siblings at successive developmental times (Fig. S4). These findings confirm the presence of a Doppler effect.

Such a Doppler effect would not occur if the wave pattern scaled (Supplementary Text). This means the wave pattern shrinks proportionally with the length of the tissue. Such a scaling of the wave pattern has been recently reported in *in vitro* cultured mouse PSM explants (5) and requires that the number of kinematic waves visible along the PSM remains constant in time. The change in number of waves observed here supports the presence of a Doppler effect and rules out scaling of the wave pattern in zebrafish.

Can we conclude that a Doppler effect alone accounts for the observed decrease in kinematic wave number and the measured period offset? In a classical Doppler effect with only the observer in motion, the wavelength of the sound waves remains constant in time (Fig. 3A). In our analogy, this would imply that the anterior end of the PSM (observer) is in motion while the local wavelength remains constant, resulting in a shortened anterior period.

However, from our phase maps, we determined that the local wavelength is not constant but decreases over time (Fig. 2C and 3B; Fig. S5, S6; Supplementary Text). This dynamic change of the wavelength tends to prolong the anterior period (Fig. 3B; Fig. S7; Supplementary text) and thus opposes the Doppler effect. Hence, the period of segmentation is modulated through the combination of these two opposing effects, the Doppler effect and the dynamic wavelength (Fig. 3C; Fig. S7). Although the relative contribution of these effects varies during development, the experimentally observed offset between anterior and posterior period is due to the larger average magnitude of the Doppler compared to the Dynamic Wavelength effect (Fig. S7; Supplementary Text). The Dynamic Wavelength effect discovered here is a general principle and there is no reason to assume it is restricted to the zebrafish PSM. An analogous effect would arise in a wave-carrying medium from a space- and time-dependent change of refraction.

Traditionally, genetic oscillations in the posterior PSM have been viewed as the pacemaker for the segmentation process, which is emphasized in the term “segmentation clock”. Our findings show that the clock metaphor is insufficient to understand the timing of segment formation. In addition to the time-scale set by the genetic network controlling the oscillations, the change in length of the PSM and the change of the kinematic wavelength must be included to understand the period of segmentation observed *in vivo*. The biological mechanisms by which the tissue length and kinematic wavelength change remain open questions. Our work highlights the need to go beyond descriptions of embryonic segmentation that are based on steady-state or scaling conditions, and reveals the consequences of the spatial features of the wave pattern for the timing of segmentation.

## Supplementary Material

Refer to Web version on PubMed Central for supplementary material.

## Acknowledgments

We thank L. Wetzel, L. Rohde, C. Poulet, C. Eugster, M. Gonzales-Gaitan, J. Firmino, for comments on the manuscript; D. Hasselhoff for mental support; and the fish and light microscopy facilities of the MPI-CBG. In memory of Julian Lewis. This work was supported by the Max Planck Society and the Medical Research Council [MC\_UP\_1202/3]; D.S., L.G.M., A.C.O. by the European Research Council (ERC) under the European Communities 7<sup>th</sup> Framework Programme [FP7/2007-2013]/[ERC grant 207634]; D.L.R. by an EMBO fellowship [ALTF1402-2011], A.C.O. and D.S. by the Wellcome Trust [WT098025MA]. The original time-lapse recordings in this study are available for anonymous download via the lab website.

## References

1. Sarrazin AF, Peel AD, Averof M. *Science*. 2012; 336:338–341. [PubMed: 22403177]
2. Delaune EA, François P, Shih NP, Amacher SL. *Dev Cell*. 2012; 23:995–1005. [PubMed: 23153496]
3. Palmeirim I, Henrique D, Ish-Horowicz D, Pourquié O. *Cell*. 1997; 91:639–648. [PubMed: 9393857]
4. Masamizu Y, et al. *Proc Natl Acad Sci USA*. 2006; 103:1313–1318. [PubMed: 16432209]
5. Lauschke VM, Tsiairis CD, François P, Aulehla A. *Nature*. 2012; 493:101–105. [PubMed: 23254931]
6. Oates AC, Morelli LG, Ares S. *Development*. 2012; 139:625–639. [PubMed: 22274695]
7. Bénazéraf B, Pourquié O. *Annu Rev Cell Dev Biol*. 2013; 29:1–26. [PubMed: 23808844]

8. Giudicelli F, Ozbudak EM, Wright GJ, Lewis J. *PLoS Biol.* 2007; 5:e150 [PubMed: 17535112]
9. Morelli LG, et al. *HFSP J.* 2009; 3:55–66. [PubMed: 19492022]
10. Soroldoni D, Oates AC. *Curr Opin Genet Dev.* 2011; 21:600–605. [PubMed: 21963131]
11. Aulehla A, et al. *Nat Cell Biol.* 2007; 10:186–193. [PubMed: 18157121]
12. Mara A, Schroeder J, Chalouni C, Holley SA. *Nat Cell Biol.* 2007; 9:523–530. [PubMed: 17417625]
13. Schroter C, et al. *Dev Dyn.* 2008; 237:545–553. [PubMed: 18265021]
14. Ozbudak EM, Lewis J. *PLoS Genet.* 2008; 4:e15 [PubMed: 18248098]
15. Sarov M, et al. *Nat Methods.* 2006; 3:839–844. [PubMed: 16990816]
16. Ejsmont R, Sarov M, Winkler S, Lipinski K, Tomancak P. *Nat Methods.* 2009; doi: 10.1038/nmeth.1334
17. Thermes V, et al. *Mech Dev.* 2002; 118:91–98. [PubMed: 12351173]
18. Soroldoni D, Hogan BM, Oates AC. *Methods Mol Biol.* 2009; 546:117–130. [PubMed: 19378101]
19. Schindelin J, et al. *Nat Methods.* 2012; 9:676–682. [PubMed: 22743772]
20. Cooke J, Zeeman EC. *J Theor Biol.* 1976; 58:455–76. [PubMed: 940335]
21. Murray PJ, Maini PK, Baker RE. *J Theor Biol.* 2011; 283:227–38. [PubMed: 21635902]
22. Quiroga, R Quian; Kraskov, A; Kreuz, T; Grassberger, P. *Phys Rev E.* 2002; 65:041903
23. Torrence C, Compo GP. *Bull Am Meteorol Soc.* 1998; 79:61–78.
24. Oates AC, Ho RK. *Development.* 2002; 129:2929–2946. [PubMed: 12050140]
25. Riedel-Kruse IH, Müller C, Oates AC. *Science.* 2007; 317:1911–1915. [PubMed: 17702912]
26. Lauter G, Söll I, Hauptmann G. *BMC Dev Biol.* 2011; 11:43. [PubMed: 21726453]

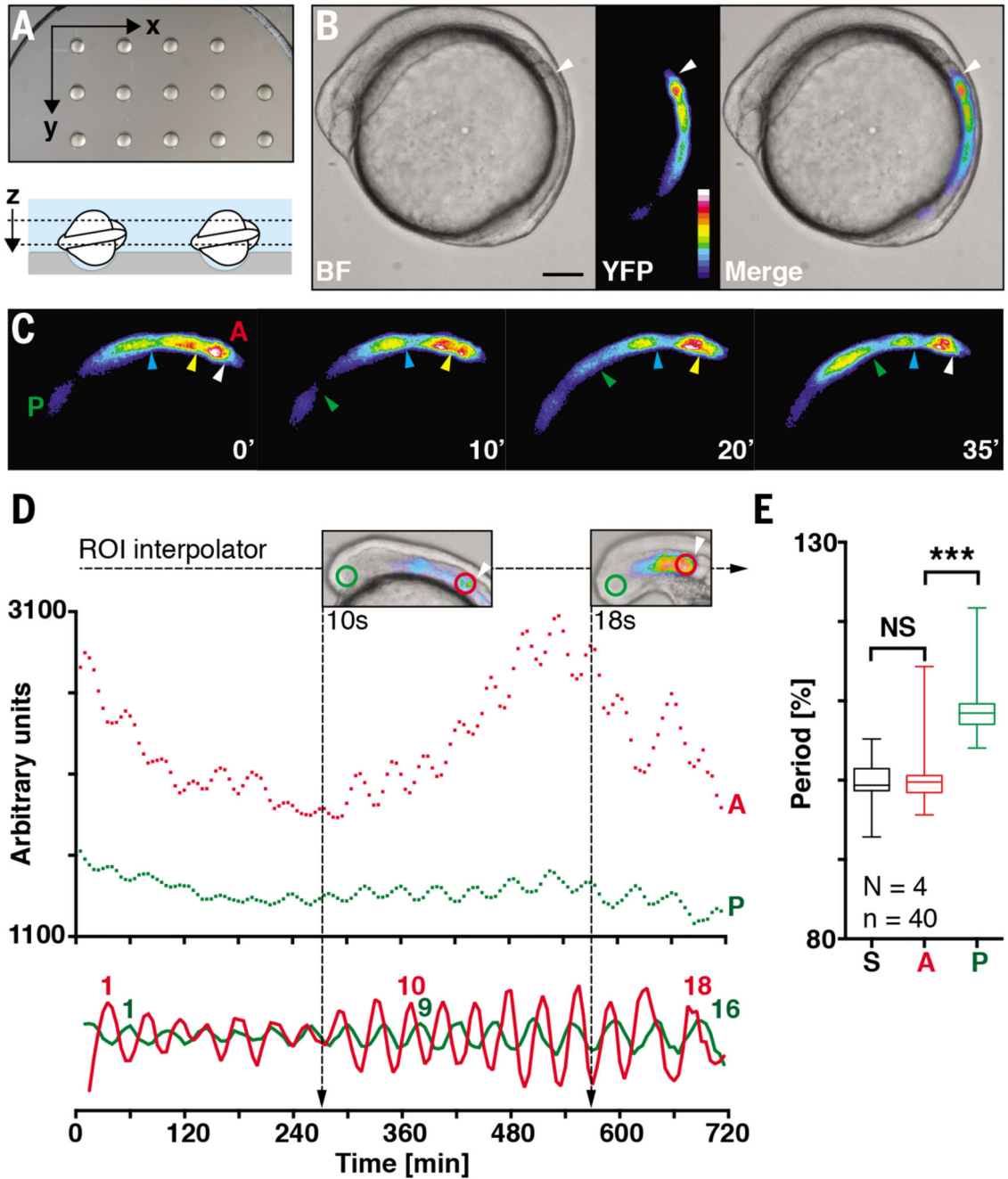


**Fig. 1. Oscillations in the anterior and posterior pre-somitic mesoderm (PSM) have different periods.**

(A) Mounting of zebrafish embryos for multidimensional imaging: Each time-lapse experiment consists of 20 *xy*-positions with a *z*-stack (6 x 20µm) to keep the PSM in focus. (B) Snapshots from *Looping*, a transgenic reporter of the oscillating gene *her1*, reveal that Her1::YFP fusion protein is confined to the PSM. The white arrowhead marks the most recently formed somite/segment boundary. Scale bar = 100 µm; LUT: high (white) to low (blue) reporter intensity; BF: brightfield (C) Multiple kinematic waves (different colored

arrowheads) emerge from the posterior PSM (P) and travel anteriorly (A) till they arrest (white arrowhead). **(D)** A region of interest (ROI) interpolator is used to measure the average reporter intensity in the posterior (inset, green circle) and anterior (inset, red circle) PSM. Both regions oscillate but experience a different number of oscillations (annotated with peak number). **(E)** Periods of morphological segmentation (S) and anterior (A) oscillations are identical whereas posterior (P) oscillations occur significantly slower (9%). Four independent experiments (N), forty individual embryos (n), Whiskers min/max, (t-test, Welch correction, \*\*\*  $p < 0.0001$ ).

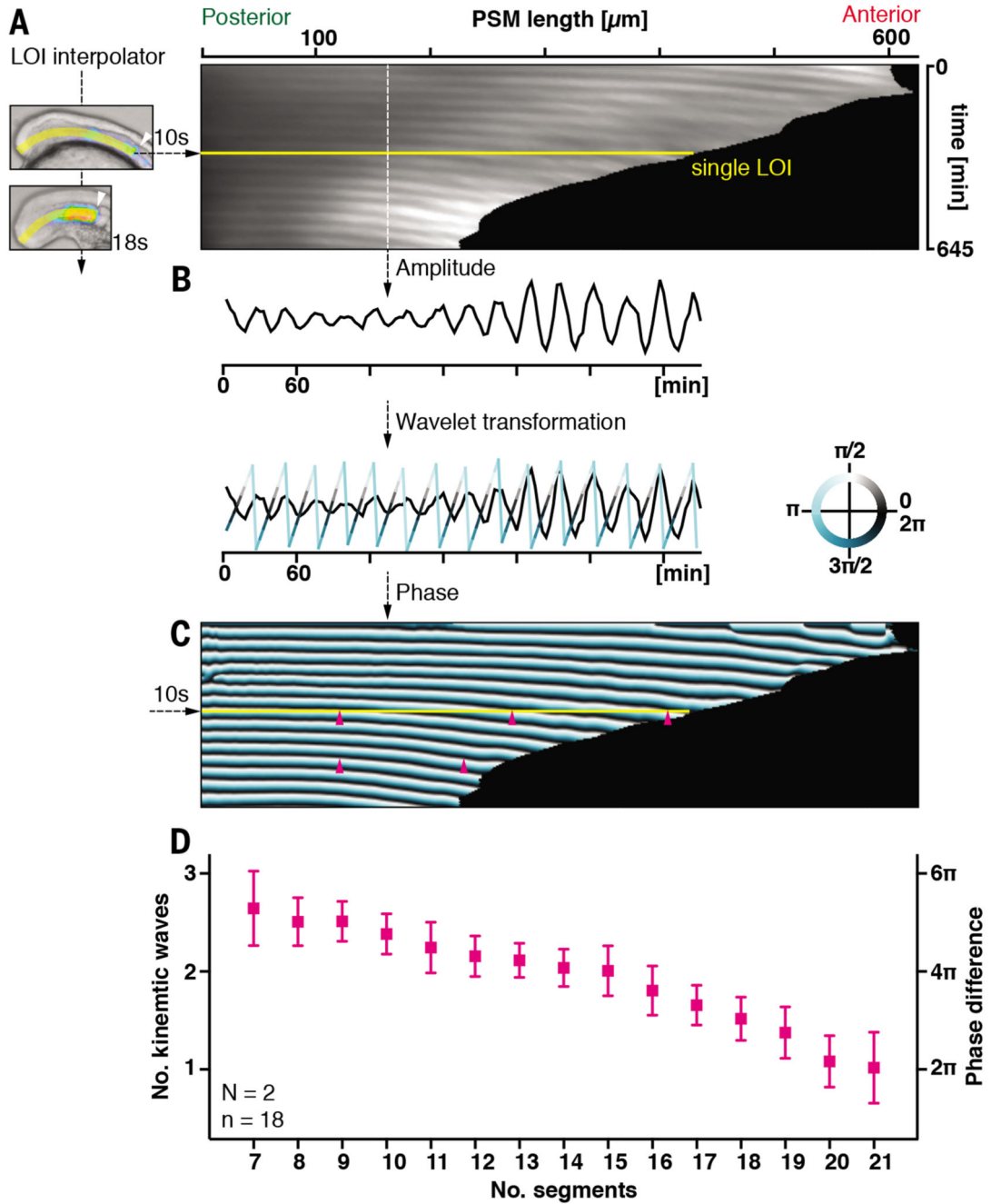


**Fig. 2. The wave pattern in the PSM changes continuously as the tissue length decreases.** (A) A line of interest (LOI) interpolator is used to measure the reporter intensity along the entire PSM and construct a kymograph that captures the trajectories of slowing, kinematic waves (tilted white ridges) and demonstrates the substantial decrease in PSM length. (B) Wavelet transformation: Each vertical line of the kymograph (white dotted line) is used to translate amplitude into phase information and construct a phase map which is independent of local amplitude fluctuations (C). A, C show a single representative embryo. Yellow horizontal lines in a phase map yields the number of kinematic waves at a given time point,



which decreases with increasing segment number (**D**). The local wavelength (distance between purple ticks) also decreases over time. Data are from two independent replicates (N), 18 embryos (n).

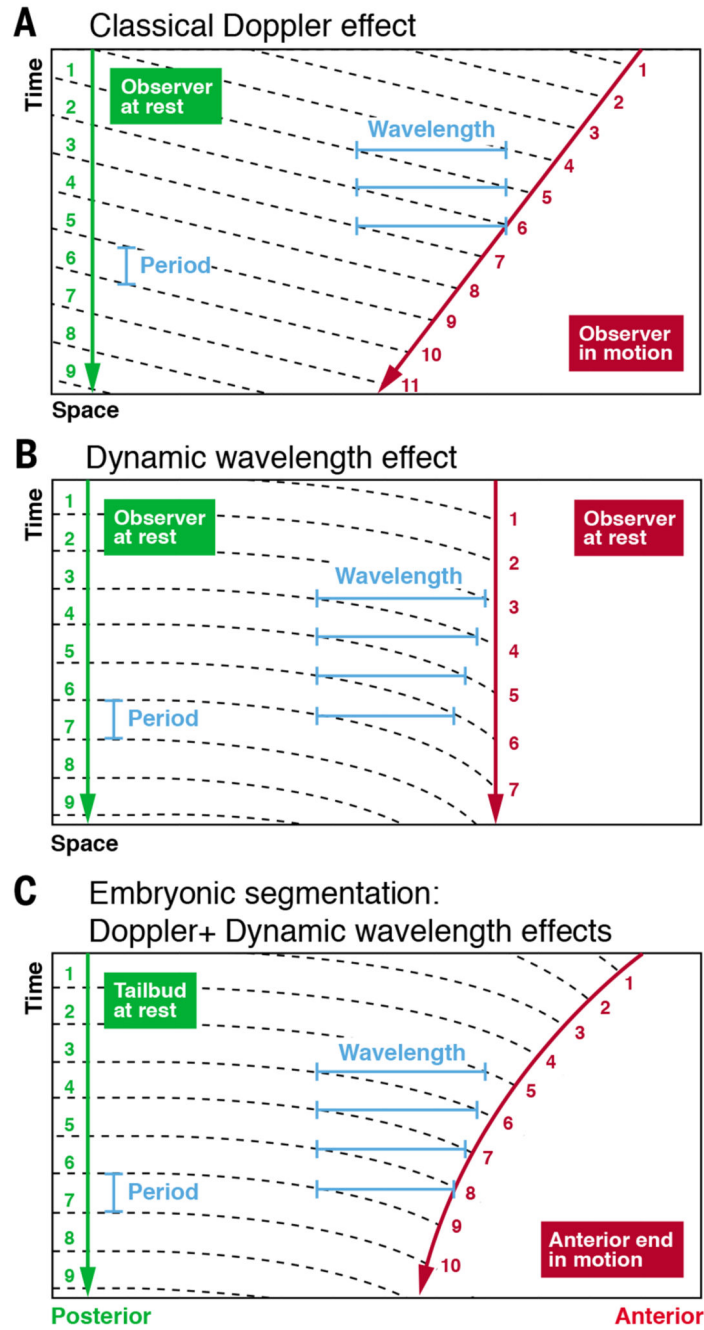


**Fig. 3. Doppler and Dynamic Wavelength effects modulate the period of segmentation.**

(A) In the classical Doppler effect an observer moving towards a sound source perceives an increased sound frequency compared to an observer at rest. This is indicated by the larger number of wave peaks (crossing dashed lines) that an observer in motion (red) experiences compared to an observer at rest (green) during the same time interval. (B) A dynamic change of the wavelength at the position of an observer at rest (red) can cause a change of the observed period compared to an observer at rest at a different position (green). (C) In the zebrafish PSM, where the anterior end acts as an observer that is moving relative to the

kinematic waves, and the wavelength is dynamically changing, these two effects combine and regulate the anterior period (compare to phase map in Fig. 2).